Single-Molecule Imaging Revealing the Deformation-Induced Formation of a Molecular Polymer Blend

Werner Trabesinger,[†] Alois Renn,[†] Bert Hecht,*[,†] Urs P. Wild,[†] Andrea Montali,[‡] Paul Smith,[‡] and Christoph Weder[‡]

Physical Chemistry Laboratory and Department of Materials, Institute of Polymers, ETH Zürich, CH-8092 Zürich, Switzerland

Received: January 14, 2000; In Final Form: April 6, 2000

Photoluminescence microscopy of conjugated polymer molecules in a polyethylene host has been applied to monitor the transition of a phase-separated polymer blend into a molecular dispersion induced by solid-state tensile deformation. Statistical analysis of conjugated polymer cluster sizes as a function of the degree of matrix deformation shows that phase-separated domains of conjugated polymer transform into smaller clusters and single molecules as the degree of matrix deformation increases. Concomitantly, the conjugated guest molecules tend to adopt the preferential orientation of the surrounding matrix. We demonstrate that single-molecule detection can be readily extended and applied to probing molecular dispersion, orientation, and morphology in polymer−polymer blends.

Introduction

Dispersions of macromolecules in a solid polymer matrix are of particular interest, because they can synergistically combine the properties of their components.[1] For example, blends of tailored properties of semiconducting conjugated polymers[2−5] and electrically inactive polymers may advantageously be used for applications in light-emitting devices,[6] transistors,[7] lasers,[8] and other optical components.[4] The functionality of such materials critically depends on their structure at the molecular level. However, molecular mixing of two polymers in general, and of rigid-rod and flexible-coil macromolecules in particular, is usually inhibited by the unfavorably low entropy of mixing.[1,9,10] In special cases, this limitation can be overcome by the preparation of copolymers[11,12] or by increasing the enthalpy of mixing, for example by introducing specific ion−ion or dipole−dipole interactions between the blend components.[13,14] In recent studies regarding the preparation of photoluminescent polarizers,[15] we surprisingly discovered that solid-state tensile deformation of initially phase-separated blends of a poly(2,5-dialkoxy-*p*-phenyleneethynylene) derivative (EHO-OPPE,[16] Figure 1) and ultrahigh molecular weight polyethylene (UHMW-PE) resulted in a material in which the conjugated species exhibited bulk photoluminescent properties that indicated an apparent molecular dispersion of the rigid-rod conjugated polymer guest in the UHMW-PE host, although a true molecular dispersion was thought to be unlikely for thermodynamic reasons.[15] Significant efforts have previously been devoted to shear-induced mixing of polymer blends.[17] However, previous work has been limited to selected, in fact rather compatible, polymer systems and compatibilization has been restricted to molten blends close to the critical point.[17] Thus, with the above-mentioned potential of "molecular composites" in mind, in particular those comprising conjugated polymers, we have undertaken a systematic investigation of this most unusual observation.

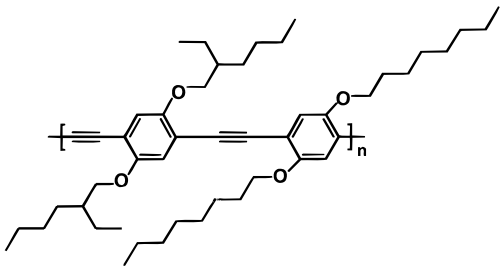

Figure 1. Chemical structure of EHO-OPPE the poly(2,5-dialkoxy-*p*-phenyleneethynylene) derivative used.

Knowledge of the structural aspects of heterogeneous polymer systems, e.g., concerning the phase behavior of polymer blends on a molecular level, is usually deduced from the interpretation of data obtained from large multimolecule ensembles such as luminescence and diffraction spectra or near-field scanning optical microscopy images.[15,16,18] Recent developments in scanning confocal optical microscopy allow for the observation of single molecules at ambient conditions,[19−22] including multichromophoric conjugated polymers[23,24] and single-molecule polarization phenomena.[25] Single-molecule detection provides a handle to investigate the interaction of single photoluminescent species with their immediate environment.[19] In contrast to ensemble measurements, single-molecule detection provides direct access to individual molecular parameters rather than ensemble averages. Measurements of absorption and emission dipole orientation[25] and diffusional trajectories[26,27] of individual absorbers have unveiled heterogeneous behavior at the level of subensembles of molecular species. Such investigations therefore reflect the inhomogeneous nature of individual molecular environments and detailed, molecular level, information on structural aspects of a chromophore−host composite can be provided.

In the present study, single-molecule analysis provides direct and detailed insight into the structural rearrangement processes that occur in the above-mentioned EHO-OPPE/UHMW-PE system. The spatial and orientational distributions as well as

* Corresponding author. E-mail: hecht@phys.chem.ethz.ch.
[†] Physical Chemistry Laboratory.
[‡] Department of Materials.

10.1021/jp000213a CCC: $19.00
Published on Web 05/11/2000

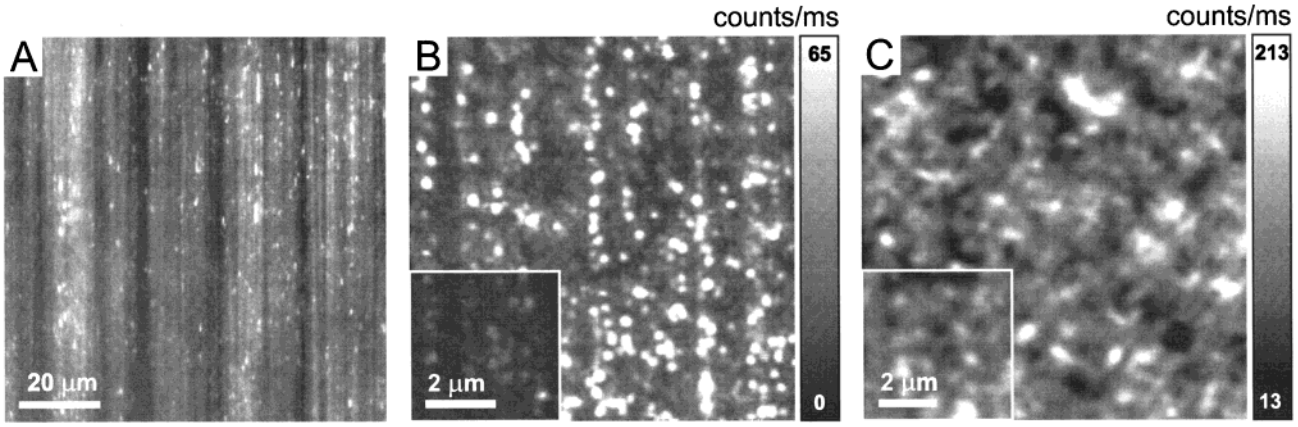

Figure 2. (A) Wide-field fluorescence image of a deformed ($\lambda = 80$, vertical direction) binary EHO-OPPE/UHMW-PE blend film comprising 2% w/w of the EHO-OPPE guest. (B) Scanning confocal optical image of a deformed ($\lambda = 80$) binary EHO-OPPE/UHMW-PE blend film comprising 10^{-4}% w/w of EHO-OPPE obtained by recording the parallel polarization component (vertical direction as in A) at an excitation intensity of 2 kW/cm^2. (C) Scanning confocal optical image of an undeformed film obtained by recording the parallel polarization component. The concentration and excitation intensity are the same as in B. Insets in B and C: images of the perpendicular polarization component recorded simultaneously at the respective positions (same scale).

the statistical occurrence of individual and clustered fluorescent conjugated polymer molecules in the material are monitored as a function of the degree of solid-state tensile deformation. Thus, an understanding of the relation between structural and functional aspects on a molecular level is obtained. Our results clearly demonstrate that single-molecule detection techniques provide a valuable tool to study relevant problems in material science on a molecular level.

Experimental Section

Sample Preparation. Samples were prepared by casting a solution of EHO-OPPE[16] (number-average molecular weight $\sim 1 \times 10^4$ g mol^{-1}; 10, 5×10^{-4}, 1×10^{-4}, and 0 mg, respectively), and UHMW-PE (Hostalen Gur 412, Hoechst AG, weight-average molecular weight $\sim 4 \times 10^6$ g mol^{-1}; 500 mg) in *p*-xylene (Fluka ppa, 50 g; dissolution at 130 °C after degassing the mixture in a vacuum at 25 °C for 15 min) into a Petri dish 11 cm in diameter. The gels were dried under ambient conditions for 24 h, leading to phase separation of the two polymers under near-equilibrium conditions. The resulting pristine films were uniaxially deformed at 120 °C to well-defined ratios λ (λ = final/initial length) of up to 80, yielding transparent films of $1-2$ μm thickness. The deformation process was conducted in the temperature window above the glass transition of the conjugated polymer (around 100 °C), and below the melting temperature of the polyethylene ($\sim$135 °C), before finally quenching the samples to room temperature. For the following optical investigation the films were embedded in silicon oil to provide index matching, and sandwiched between a microscopy slide and a cover glass.

Microscopy. Binary blend films and neat UHMW-PE reference samples of different deformation ratios λ were investigated using standard fluorescence wide-field and fluorescence scanning confocal optical microscopy[28] to image samples with a high and low concentration of conjugated polymer, respectively. The wide-field fluorescence microscope (Leica) was equipped with a UV lamp in combination with a suitable filter block (Leica, $I^2/_3$). For confocal microscopy, EHO-OPPE was excited using circularly polarized laser light at a wavelength of 488 nm focused to a diffraction-limited spot by an immersion oil microscope objective (Zeiss, 1.4 NA, ∞). EHO-OPPE fluorescence was collected by the same objective and directed via a dichroic mirror and a cutoff filter ($\sim$520 nm) toward a polarizing beam splitter. The resulting orthogonal components of the fluorescence are detected by two single-photon counting avalanche diodes. Images are generated by scanning the sample by means of a linearized $x-y-z$ piezo scan table and recording the number of counts for each pixel. In all experiments the sample was oriented such that the detectors record the component parallel or perpendicular to the direction of tensile deformation, respectively.

Results and Discussion

Wide-Field Imaging. Figure 2A shows a 100×100 μm^2 wide-field fluorescence image of a deformed ($\lambda = 80$) binary blend film containing 2% w/w EHO-OPPE. Highly fluorescent, stripe-like structures are observed with intermittent darker elongated domains oriented parallel to the stretching direction. The latter coincides with the preferential polarization of the fluorescence emission.[15] This observation is strongly supported by earlier photoluminescence, X-ray, and electron diffraction experiments which indicated that the macroscopic tensile deformation leads to a "breaking up" and "smearing out" of the originally phase-separated EHO−OPPE clusters accompanied by an increasingly polarized fluorescence emission.[15]

Confocal Imaging. Figure 2, B and C, shows typical polarized fluorescence images of a stretched ($\lambda = 80$) and an unstretched dilute (10^{-4}% w/w EHO−OPPE) binary blend film, respectively, recorded by detecting the polarization component parallel to the deformation direction. Most strikingly, Figure 2B exhibits well-separated diffraction-limited fluorescent spots of variable intensity, organized in rows along the direction of tensile deformation. Many of these spots can be attributed to single EHO-OPPE molecules because of their characteristic blinking and stepwise photobleaching apparent from fluorescence time traces[29] in Figure 3A. These observations were absent for the unstretched film (Figure 2C), consistent with the presence of large EHO-OPPE clusters in the latter that are phase-separated from the UHMW-PE matrix. The insets in Figure 2B,C show the fluorescence signal recorded simultaneously for the perpendicular polarization component at the corresponding positions. The large difference in average fluorescence intensity between the polarization directions in Figure 2B clearly demonstrates on a molecular level the high degree of orientation of the conjugated molecules in the spots. This is in sharp contrast to the corresponding confocal images of the undeformed film

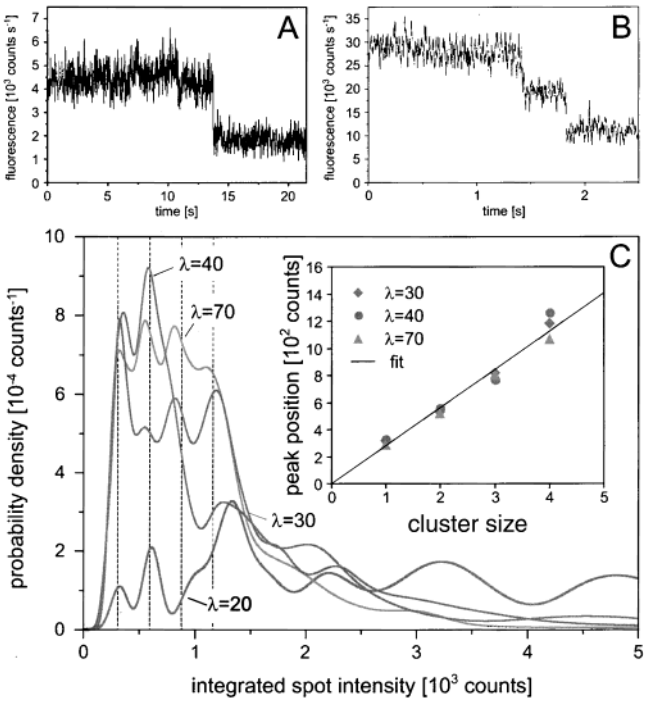

Figure 3. (A,B) Fluorescence time traces of deformed binary EHO-OPPE/UHMW-PE blend films ($\lambda = 80$) comprising 10^{-4}% w/w of the EHO-OPPE guest, recorded at an excitation intensity of 2 and 12 kW/cm^2, respectively. The traces suggest the presence of one (A) and two chromophores (B), respectively. (C) Intensity probability density functions (pdf's) of deformed binary EHO-OPPE/UHMW-PE blend films comprising 10^{-4}% w/w of the EHO-OPPE guest, as a function of λ. The inset shows a plot of the average integrated cluster intensity vs assigned cluster size (the pdf for the $\lambda = 20$ film is omitted because the uni- and bichromophoric peaks are due to only one fluorescence spot and the ter-chromophoric peak happens to be completely absent).

(Figure 2C and inset) where equal intensities are observed for both polarizations. Reference samples without EHO-OPPE show only very weak fluorescence, well below the count rate of typical single conjugated polymer fluorescence spots. The number of fluorescent spots observed in the oriented blends was found to scale linearly with the nominal concentration of conjugated polymer, but typically accounted for only about 12% of the nominal EHO-OPPE concentration. This finding is in agreement with previous single-molecule studies of conjugated polymers[23,24] and is consistent with the existence of nonluminescent molecules, an uncertainty in molecular weight of EHO-OPPE, and actual losses of the latter during sample preparation.

Additional time traces acquired on fluorescence spots in the deformed films often show bleaching in several steps of equal intensity (Figure 3B), suggesting that the brighter spots observed in Figure 2B represent clusters of multiple chromophores. Interestingly, the degree of deformation-induced orientation appeared to be a function of cluster size. Weaker spots, in general, were found to be predominantly visible in the parallel polarization image (compare Figure 2B and inset), consistent with a high degree of orientation of the respective chromophores. More intense spots, on the contrary, show the tendency to be also visible in the perpendicular polarization direction, indicating a reduced orientation of the EHO-OPPE molecules when clustered.

Quantitative Analysis. In order to obtain more quantitative information on the degree of clustering and orientation of single EHO-OPPE molecules as a function of deformation ratio, large areas ($\sim 25 \times 25\ \mu$m^2) of stretched films (10^{-4}% w/w EHO-OPPE) were imaged by scanning confocal optical microscopy. A nonlinear least-squares fit of fluorescence spots in the images to two-dimensional Gaussians was performed using the Levenberg−Marquard algorithm[30] which determines their center, integrated intensity, the local background, and the respective errors. All subsequent statistical evaluations were based on fluorescent spots with a peak height exceeding the local background by a factor of at least 3, and which met the additional requirement that the error[30] of the intensity parameter did not exceed 20% of the integrated peak intensity. By applying these two empirical criteria, fits of poor quality in areas with large background signal, or due to photobleaching, are discarded without introducing a bias for any particular cluster size. Each fitted fluorescence spot permits the construction of a probability density function (pdf) that specifies the probability for possible results of repeated integrated intensity measurements on the same spot.[31] Combining all individual pdfs for accepted fluorescence spots (typically about 100 for a given λ) results in pdfs that characterize the probability distribution for measuring a certain integrated intensity on a randomly selected fluorescent spot. Figure 3C shows such combined pdfs for films of various draw ratios. At smaller integrated intensities, the combined pdfs show, independent of λ, well-defined equidistant maxima (inset Figure 3C), evidencing the presence of an integer number of chromophores in each cluster. The total probability for measuring a given cluster size (i.e., the number of chromophores comprising a cluster) can be deduced from such combined pdfs by fitting with a sum of Gaussians yielding peak positions and relative weight of the first four peaks.[31] Clusters with a size >4 cannot be unambiguously assigned to an integer multiple of the basic intensity while, however, still contributing to the pdf with the appropriate statistical weight. This behavior is related to an increasing error in the intensity measurement, due to increased photobleaching probability and energy-transfer effects in larger clusters, and an intrinsic broadening of individual pdfs due to shot noise.[31] We monitored the relative weight of the different cluster sizes to study cluster dispersion as a result of tensile deformation. The obvious increase in the occurrence of single chromophores and bichromophoric clusters with increasing deformation ratio (Figure 3C) at the expense of the number of larger clusters illustrates the increased degree of molecular dispersion of initially phase-separated domains. This effect is illustrated by comparing, for example, the combined pdfs for $\lambda = 30$ and $\lambda = 40$. The probability to find single chromophores and bichromophoric clusters is strongly increased for the latter. For the $\lambda = 70$ combined pdf, a strong decrease in the statistical weight of larger clusters is observed, while the weight of the first three peaks is approximately equal. The statistical weight of single chromophores and bichromophoric clusters in the latter sample is actually slightly smaller than for $\lambda = 40$. We attribute this finding to minor local inhomogeneities in the films that could not completely be averaged out, although at least two images recorded at different locations were evaluated. However, the combination of additional wide-field fluorescence and scanning confocal optical images suggests that the presently employed (unstretched as well as stretched) dilute blend films are, on a large scale, rather homogeneous with respect to size and distribution of EHO-OPPE clusters. Thus, the results obtained from scanning confocal optical images seem to adequately reflect the "average structure" of the films and Figure 3C provides clear quantitative evidence for a deformation-induced molecular dispersion of small clusters, ultimately leading to blends that comprise a significant fraction of isolated single chromophores.

Deformation-Induced Orientation. To address the issue of deformation-induced orientation of the molecules, the average

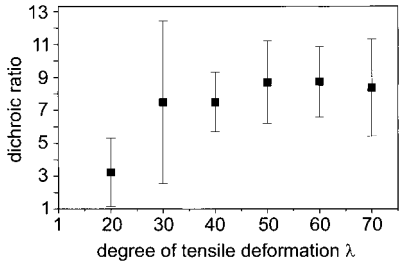

Figure 4. Average dichroic ratio of individual EHO-OPPE clusters and single molecules in deformed binary EHO-OPPE/UHMW-PE blend films comprising 10^{-4}% w/w of the EHO-OPPE guest, as a function of λ. The maximum dichroic ratio that can be observed on the level of single molecules is limited here by the nonnegligible contribution of background luminescence and is therefore smaller than in macroscopic studies.[15]

dichroic ratio of isolated fluorescence spots was determined as a function of λ by dividing the integrated intensities of fluorescence spots occurring at the same position in the two orthogonally polarized fluorescence images. The results, which are obtained for the same set of fluorescence spots as used for Figure 3, are plotted in Figure 4. Gratifyingly, the dichroic ratio increases with increasing draw ratio and reaches saturation around $\lambda = 40$, in perfect accord with results obtained in previous macroscopic studies,[15] and also the dispersion behavior reflected by Figure 3C.

Conclusion

We were able to monitor the results of molecular rearrangements taking place during the solid-state tensile deformation of an initially phase-separated polymer blend. At the example of EHO-OPPE in polyethylene we demonstrate at the level of single molecules that tensile deformation can lead to a molecular dispersion of highly incompatible polymers. Concomitantly, during deformation, the conjugated polymer adopts the orientation of its host. Our results clearly demonstrate the fundamentally new experimental possibilities that arise from a combination of single-molecule analysis with polymer science and technology. The methods presented here can be readily transferred to a variety of other relevant problems in material science thus opening the road to a molecular level understanding of the functionality of complex polymeric materials.

Acknowledgment. We thank Dr. Theo Tervoort for very helpful discussions.

References and Notes

(1) Utracki, L. A. *Polymer alloys and blends: Thermodynamics and rheology*, Carl Hanser Verlag: München, Germany, 1989.

(2) Vestweber, H.; Oberski, J.; Greiner, A.; Heitz, W.; Mahrt, R. F.; Bässler, H. *Adv. Mater. Opt. Electron.* **1993**, *2*, 197.

(3) Granström, M.; Inganäs, O. *Appl. Phys. Lett.* **1996**, *68*, 147.

(4) Weder, C.; Sarwa, C.; Montali, A.; Bastiaansen, C.; Smith, P. *Science* **1998**, *279*, 835.

(5) Montali, A.; Bastiaansen, C.; Smith, P.; Weder, C. *Nature* **1998**, *392*, 261.

(6) Burroughs, J. H.; Bradley, D. D. C.; Brown, A. R.; Marks, R. N.; Mackay, K.; Friend, R.; Burn, P. L.; Holmes, A. B. *Nature* **1990**, *347*, 539.

(7) Burroughs, J. H.; Jones, C. A.; Friend, R. H. *Nature* **1988**, *335*, 137.

(8) Tessler, V.; Denton, G. J.; Friend, R. *Nature* **1996**, *382*, 695.

(9) Flory, P. J. *Macromolecules* **1978**, *11*, 1138.

(10) Koningsveld, R.; Stockmayer, W. H.; Nies, E. *Polymer Phase Diagrams*; Oxford University Press: London, in press.

(11) Gieselman, M. B.; Reynolds, J. R. *Macromolecules* **1990**, *23*, 3118.

(12) Lauter, U.; Meyer, W. H.; Wegner, G. *Macromolecules* **1997**, *30*, 2092.

(13) Eisenbach, C. D.; Hofmann, J.; Fischer, K. *Macromol. Rapid. Commun.* **1994**, *15*, 117. Eisenbach, C. D.; Hofmann, J.; MacKnight, W. J. *Macromolecules* **1994**, *27*, 3162.

(14) Wirtz, D.; Werner, D. E.; Fuller, G. G. *J. Chem. Phys.* **1994**, *101*, 1679.

(15) Weder, C.; Sarwa, C.; Bastiaansen, C.; Smith, P. *Adv. Mater.* **1997**, *9*, 1035.

(16) Weder, C.; Wrighton, M. S. *Macromolecules* **1996**, *29*, 5157.

(17) Van Egmond, J.; Fuller, G. G. *Macromolecules* **1993**, *26*, 7182. Kim, S.; Hobbie, E. K.; Yu, J.-W.; Han, C. C. *Macromolecules* **1997**, *30*, 8245. Sundararaj, U.; Macosko, C. W. *Macromolecules* **1995**, *28*, 2647. Levitt, L.; Macosko, C. W.; Pearson, S. D. *Polym. Eng. Sci.* **1996**, *36*, 1647.

(18) Hsu, J. H.; Wei, P. K.; Fann, W. S.; Chuang, K. R.; Chen, S. A. *Ultramicroscopy* **1998,** *71*, 263. Webster, S.; Smith, D. A.; Batchelder, D. N.; Lidzey, D. G.; Bradley, D. D. C. *Ultramicroscopy* **1998,** *71*, 275. DeAro, J. A.; Weston, K. D.; Buratto, S. K.; Lemmer, U. *Chem. Phys. Lett.* **1997**, *277*, 532.

(19) Xie, X. S.; Trautman, J. K. *Annu. Rev. Phys. Chem.* **1998**, *49*, 441. Frontiers in Chemistry: Single Molecules. *Science* **1999**, *283*. Basche, T.; Moerner, W. E.; Orrit, M.; Wild, U. P. *Single-molecule optical detection, imaging and spectroscopy* VCH: Weinheim, Germany, 1997.

(20) Macklin, J. J.; Trautman, J. K.; Harris, T. D.; Brus, L. E. *Science* **1996**, *272*, 255.

(21) Lu, H.; Xie, X. S. *Nature* **1997**, *385*, 143.

(22) Nie, S.; Chiu, D. T.; Zare, R. N. *Science* **1994**, *266*, 1018.

(23) Vanden Bout, D. A.; Yip, W.-T.; Hu, D.; Fu, D.-K.; Swager, T.; Barbara, P. F. *Science* **1997**, *277*, 1074.

(24) Yip, W.-T.; Hu, D.; Yu, J.; Vanden Bout, D. A.; Barbara, P. F. *J. Phys. Chem. A* **1998**, *102*, 7564. Hu, D.; Yu, J.; Barbara, P. F. *J. Am. Chem. Soc.* **1999**, *121*, 6936.

(25) Betzig, E.; Chichester, R. J. *Science* **1993**, *262*, 1422. Ha, T.; Enderle, T.; Chemla, D. S.; Selvin P. R.; Weiss, S. *Phys. Rev. Lett.* **1996**, *77*, 3979. Sepiol, J.; Jasny. J.; Keller, J.; Wild, U. P. *Chem. Phys. Lett.* **1997**, *273*, 444−448. Ha, T.; Glass, J.; Enderle, T.; Chemla, D. S.; Weiss, S. *Phys. Rev. Lett.* **1998**, *80*, 2093. Dickson, R. M.; Norris, D. J.; Moerner, W. E. *Phys. Rev. Lett.* **1998**, *81*, 5322. Empedocles, S. A.; Neuhauser, R.; Bawendi, M. G. *Nature* **1999**, *399*, 126. Bartko, A. P.; Dickson, R. M. *J. Phys. Chem. B* **1999**, *103*, 11237

(26) Schmidt, T.; Schütz, G. J.; Baumgartner, W.; Gruber, H. J.; Schindler, H. *Proc. Natl. Acad. Sci. U.S.A.* **1996**, *93*, 2926. Dickson, R. M.; Norris, D. J.; Tzeng, Y.-L.; Moerner, W. E. *Science* **1996**, *274*, 966.

(27) Bopp, M. A.; Meixner, A. J.; Tarrach, G.; Zschokke-Granacher, I.; Novotny, L. *Chem. Phys. Lett.* **1996**, *263*, 721.

(28) Fleury, L.; Sick, B.; Zumofen, G.; Hecht, B.; Wild, U. P. *Mol. Phys.* **1998**, *95*, 1333.

(29) Fluorescence time traces were recorded by positioning well-isolated fluorescence spots in the confocal volume and directing the fluorescence counts to a multichannel analyzer.

(30) Bevington, P. R.; Robinson, D. K. *Data reduction and error analysis for the physical sciences*; McGraw-Hill: New York, 1994.

(31) Schmidt, T.; Schütz, G. J.; Gruber, H. J.; Schindler, H. *Anal. Chem.* **1996**, *68*, 4397.